PS Organic Matter Deformation in Overmature Mudrocks*

Guochang Wang[1]

Search and Discovery Article #51571 (2019)**
Posted May 27, 2019

*Adapted from poster presentation given at 2018 AAPG 47th Annual AAPG-SPE Eastern Section Joint Meeting, Pittsburgh, Pennsylvania, October 7-11, 2018
 DOI:10.1306/51571Wang2019

[1]Engineering Department, Saint Francis University, Loretto, PA (gwang@francis.edu)

Abstract

Pores within organic matter (OM) are strongly linked to hydrocarbon generation and primary migration in fine-grained source rocks and are very important for evaluating hydrocarbon storage and flow in shale reservoirs. Under overmature stage, abundant pores are formed within the OM. The porous and ductile OM should be deformed when the original equilibrium of stress condition is altered. OM deformation at the nano- or micro-scale has rarely been discussed due to the lack of associated evidence. This research documents evidence of OM deformation observed in scanning electron microscope (SEM) images of seven overmature samples from the Longmaxi Shale, Sichuan Basin. Deformation processes of OM-hosted pores were qualitatively analyzed with assumptions. To further discuss the features of OM deformation and its effect on OM-hosted pores, the OM deformation is classified into three types (I, II, and III) according to the amount of additional forces, and deformation sub-types are recognized according to the contact area of OM particles and mineral grains along which the additional force applied to the OM and overlapping of displacement fields. Two OM particles subjected to Type I deformation were analyzed quantitatively for such parameters as pore size, geometry, and orientation of long axes of elliptical pores. The reduction of OM-hosted pore volume, specific surface area, and organic porosity was calculated using the two OM particles suffering from Type I deformation.

References Cited

Dong, T., N.B. Harris, K. Ayranci, Korhan, C.E. Twemlow, and B.R. Nassichuk, 2017, The Impact of Composition on Pore Throat Size and Permeability in High Maturity Shales: Middle and Upper Devonian Horn River Group, Northeastern British Columbia, Canada: Marine and Petroleum Geology, v. 81, p. 220-236. doi.10.1016/j.marpetgeo.2017.01.011

Jiao, K., S. Yao, C. Liu, G. Yuqiao, H. Wu, M. Li, and Z. Tang, 2014, The Characterization and Quantitative Analysis of Nanopores in Unconventional Gas Reservoirs Utilizing FESEM–FIB and Image Processing: An example from the Lower Silurian Longmaxi Shale, Upper Yangtze Region, China: International Journal of Coal Geology, v. 128-129, p. 1-11. doi.10.1016/j.coal.2014.03.004

Klaver, J., G. Desbois, R. Littke, and J.L. Urai, 2015, BIB-SEM Characterization of Pore Space Morphology and Distribution in Postmature to Overmature Samples from the Haynesville and Bossier Shales: Marine and Petroleum Geology, v. 59, p. 451-466. doi.org/10.1016/j.marpetgeo.2014.09.020

Loucks, R.G., R.M. Reed, S.C. Ruppel, and D.M. Jarvie, 2009, Morphology, Genesis, and Distribution of Nanometer-Scale Pores in Siliceous Mudstones of the Mississippian Barnett Shale: Journal of Sedimentary Research, v. 79/12, p. 848-861. doi.org/10.2110/jsr.2009.092

Milliken, K., M. Rudnicki, D.N. Awwiller, and T. Zhang, 2013, Organic Matter-Hosted Pore System, Marcellus Formation (Devonian), Pennsylvania: American Association of Petroleum Geologists Bulletin, v. 97. P. 177-200. doi.10.1306/07231212048.

Peng, S., J. Yang, X. Xiao, R.G. Loucks, S.C. Ruppel, and T. Zhang, 2015, An Integrated Method for Upscaling Pore-Network Characterization and Permeability Estimation: Example from the Mississippian Barnett Shale: Transport in Porous Media, v. 109/2, p. 359-376. doi.10.1007/s11242-015-0523-8

Schieber, J., 2010, Common Themes in the Formation and Preservation of Porosity in Shales and Mudstones: Illustrated with Examples Across the Phanerozoic: SPE Unconventional Gas Conference, 23-25 February, Pittsburgh, Pennsylvania, USA, SPE-132370-MS, 10 p. doi.org/10.2118/132370-MS

2018 Joint Eastern Section AAPG/SPE Conference in Pittsburgh, PA

Organic Matter Deformation in Overmature Mudrocks

Guochang Wang
Engineering Department, Saint Francis University, Loretto, PA 15940, USA

❖ Introduction

Pores within organic matter (OM) are strongly linked to hydrocarbon generation and primary migration in fine-grained source rocks and are very important for evaluating hydrocarbon storage and flow in shale reservoirs. Along with hydrocarbon generation, abundant pores are formed within the OM. The porous and ductile OM should be deformed when the original equilibrium of stress condition is altered. OM deformation at the nano- or micro-scale has rarely been discussed due to the lack of associated evidence. This research documents evidence of OM deformation observed in scanning electron microscope (SEM) images of seven overmature samples from the Lower Silurian Longmaxi Shale, Sichuan Basin.

❖ Assumptions of OM-hosted Pores

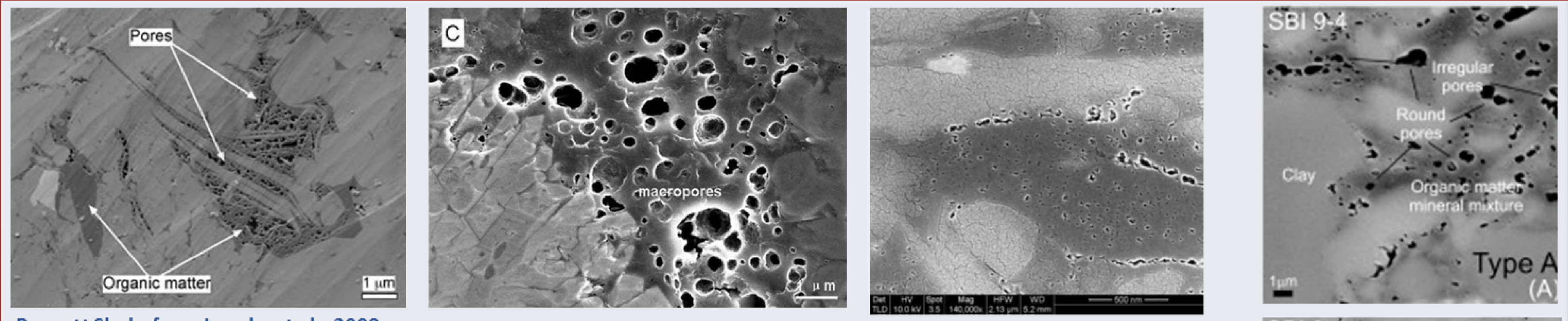

Barnett Shale from Loucks et al., 2009
Horn River Fm from Dong et al., 2017
Marcellus Shale from Milliken et al., 2013

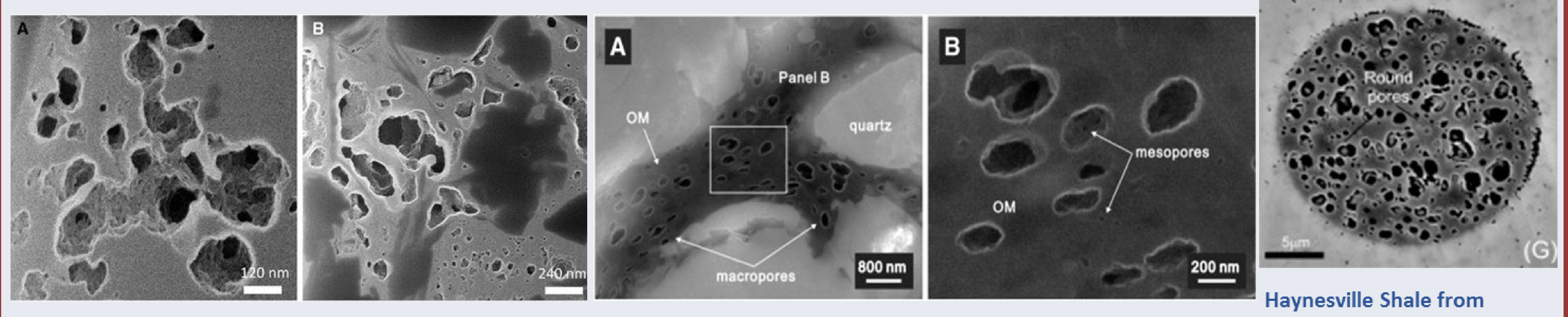

Barnett Shale from Peng et al., 2015
Longmaxi Shale from Jiao et al., 2014
Haynesville Shale from Klaver et al., 2015

- Based on these SEM images, assumptions are proposed for OM-hosted pores within bitumen
  - OM-hosted pores usually have a ***random distribution*** of size and orientation
  - The geometry of OM-hosted pores is ***spherical or near spherical*** with smooth walls
- As thermal maturity increases, OM-hosted pores will form and grow larger, causing the pores merging together

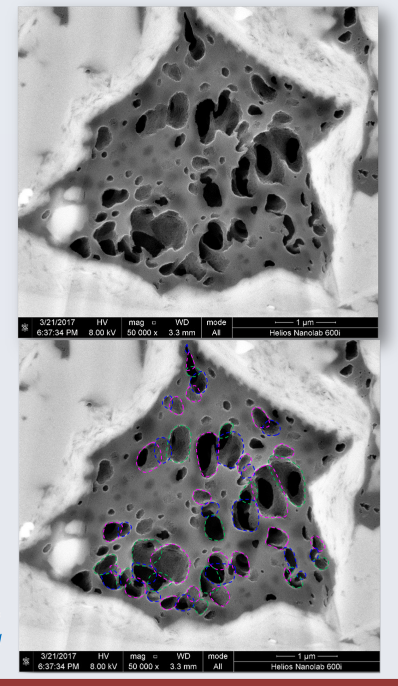

Sample A02

❖ OM Deformation Evidence

The size and orientation of OM-hosted pores are NOT randomly distributed in the sample shown below. As closing to the purple-highlighted minerals,

- the pore size becomes smaller,
- pore orientation tends to follow the mineral boundary,
- and pores become more flat.

Sample A03

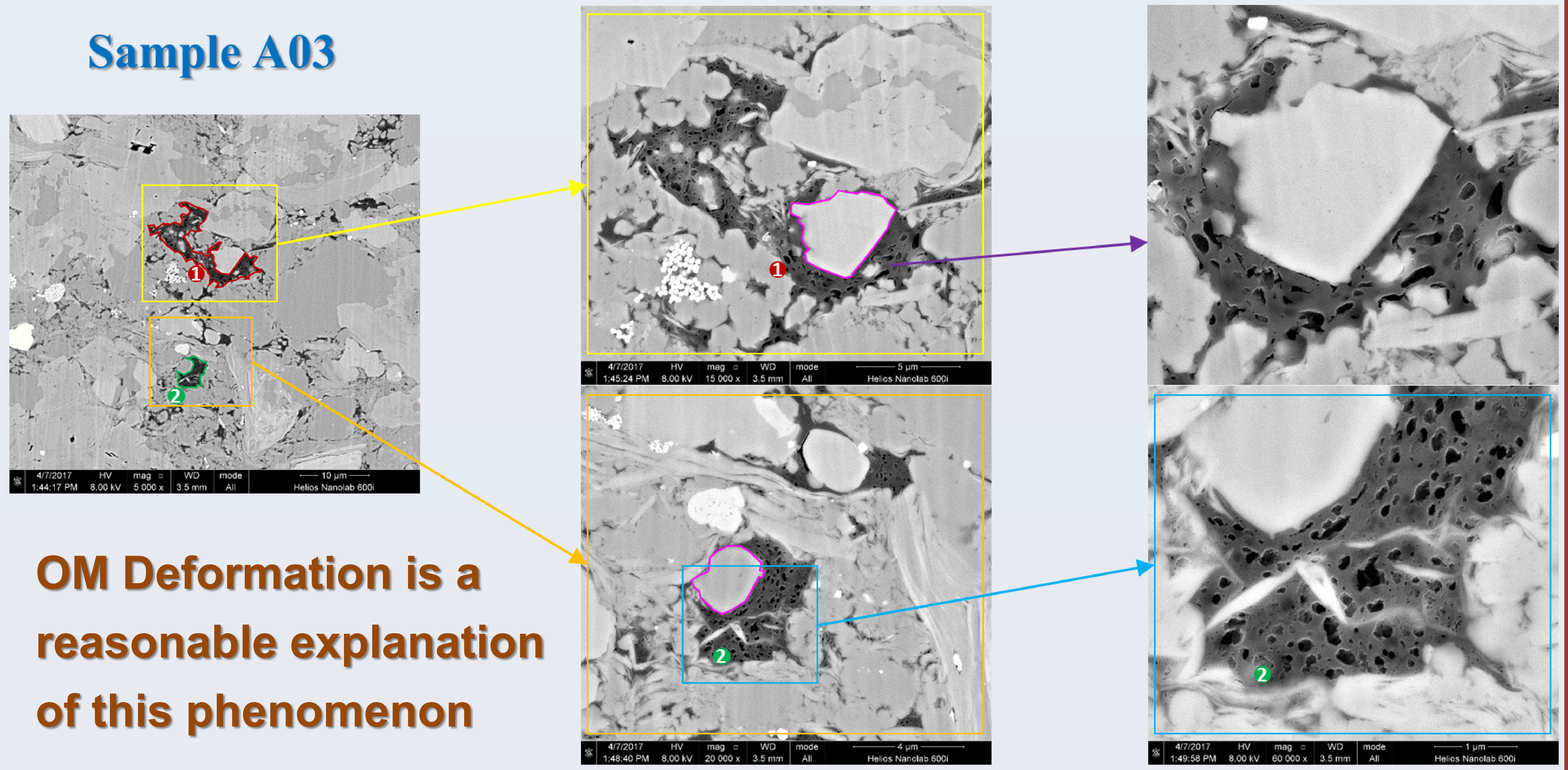

OM Deformation is a reasonable explanation of this phenomenon

Therefore, the pores within bitumen are used as a gauge or reference for OM deformation. More examples of the deformed OM particles from Longmaxi Shale are shown below: partial deformation or complete deformation.

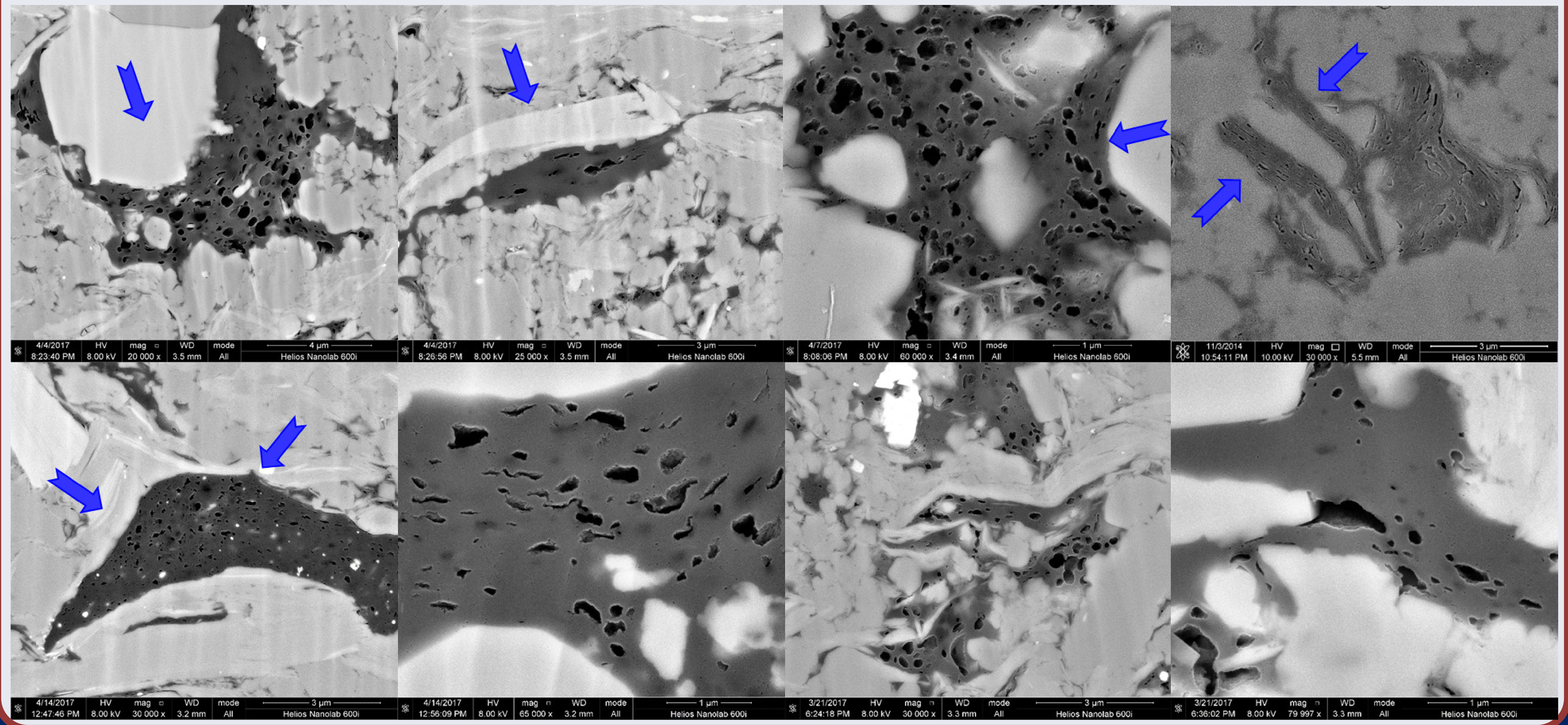

❖ Method of Quantitative Evaluation of Deformed OM-hosted Pores

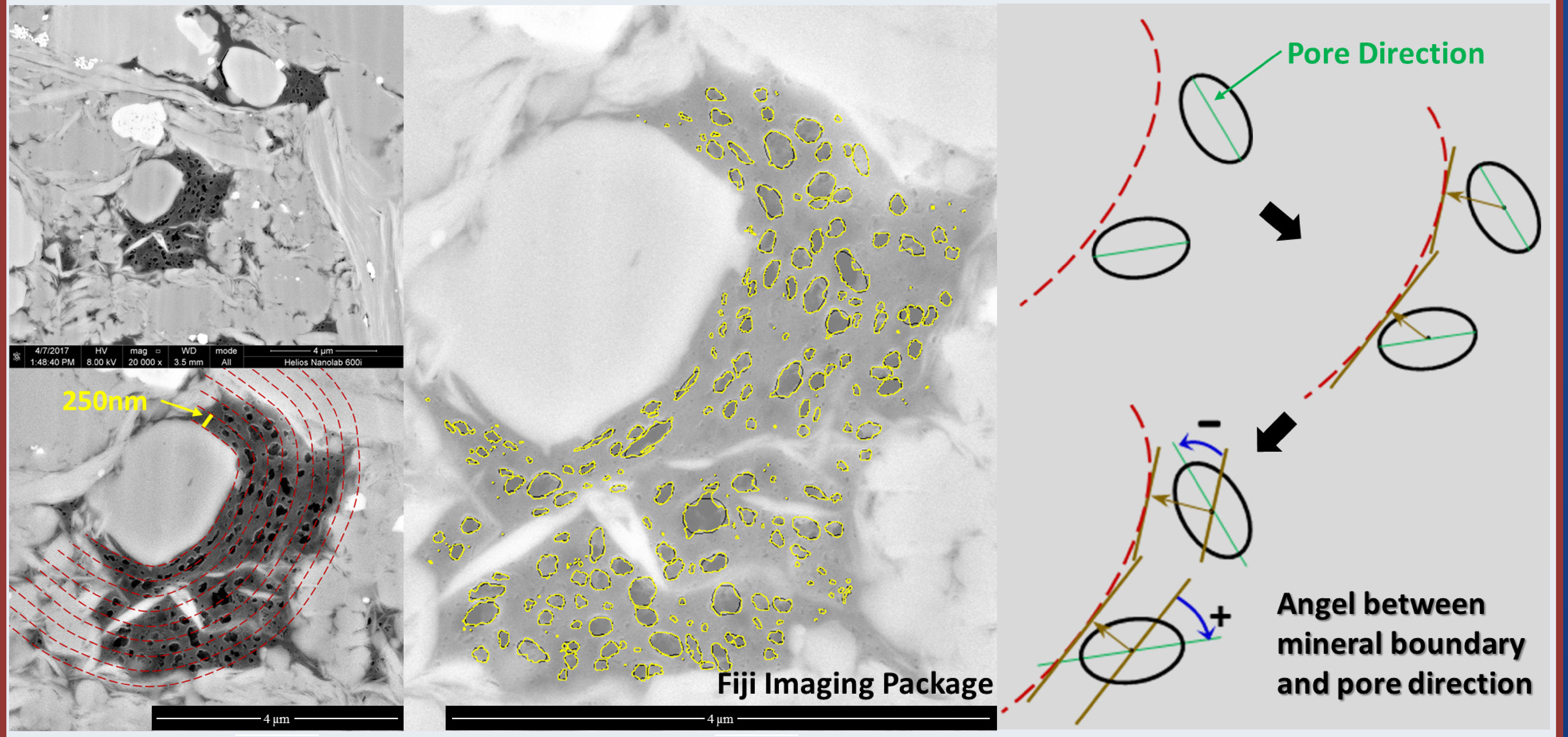

OM particle was divided into multiple regions based on distance to the boundary of the mineral that transferred the additional force to the OM (8 regions with 250nm width). Angel between mineral boundary and direction of major axis of pores was calculated with aids from Fiji Software.

❖ Quantitative Estimate of OM-hosted Pore Orientation

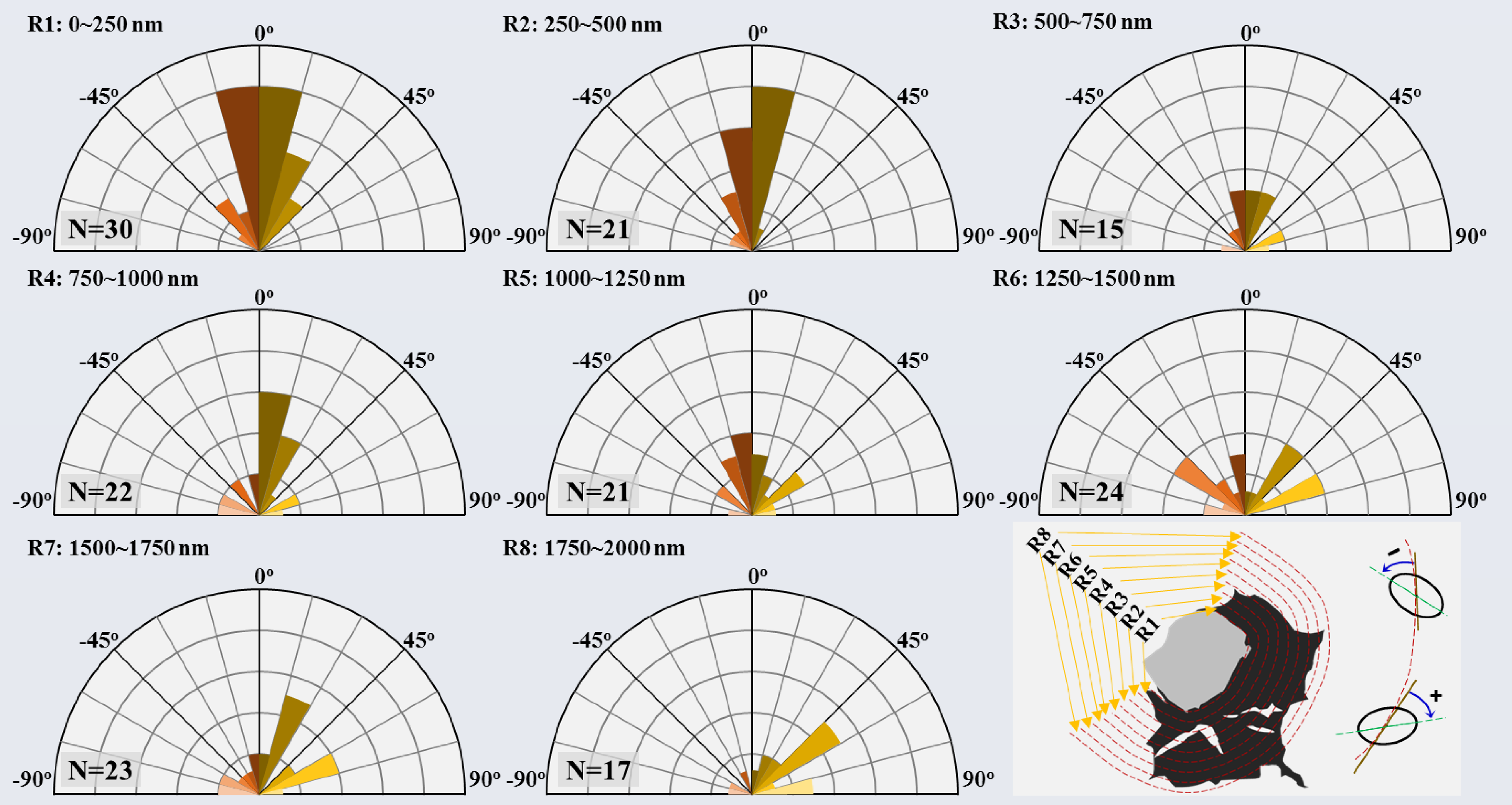

❖ Quantitative Estimate of OM-hosted Pore Size and Geometry

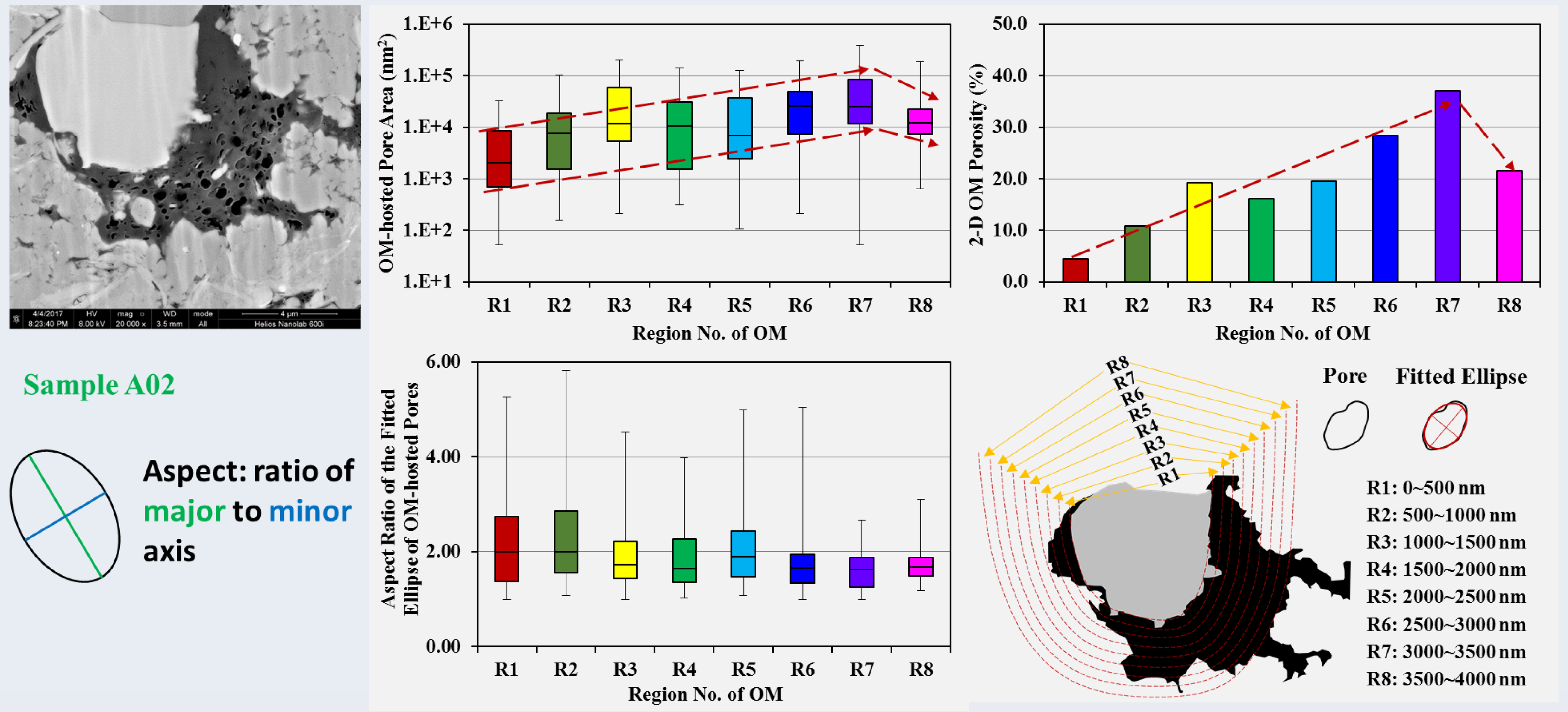

❖ Nanoscale Stress Heterogeneity within Mudrocks

OM Type includes

- **Kerogen (*Sedimentary OM*): Type I, II and III--Solid**
- **Bitumen (*Released Liquid*)—Solid/Quasi-Solid**

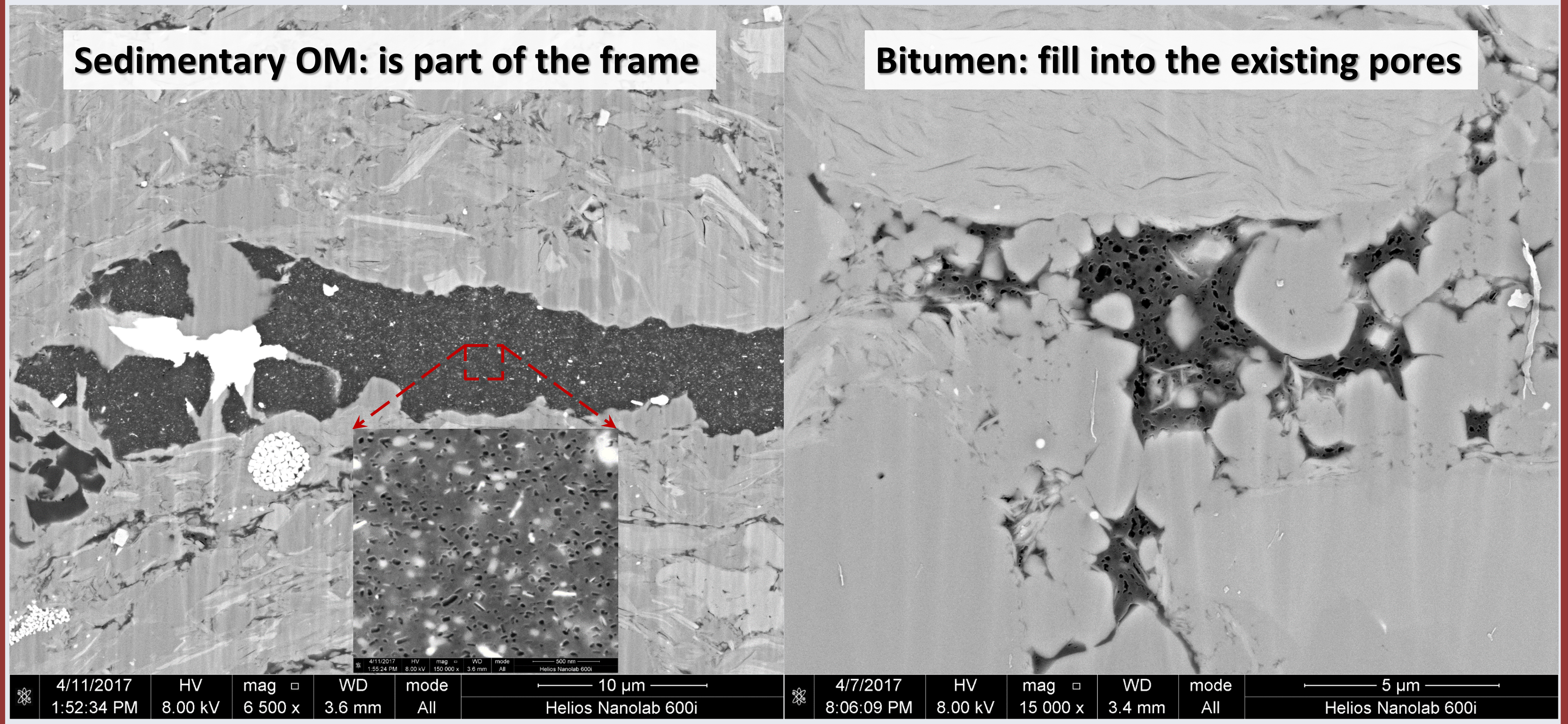

Stress shadow results form the discrete grains which generate the framework with stress resistance. The stress shadow causes difference of OM deformation among OM particles within a small area (about µm²) and within a single OM particle.

❖ Classification of OM Deformation

Deformation is classified into three types according to kinematic arrangement of deforming forces, and each type is subdivided based on the nature of contact surfaces of OM particles and mineral grains along which forces in excess of hydrostatic are applied.

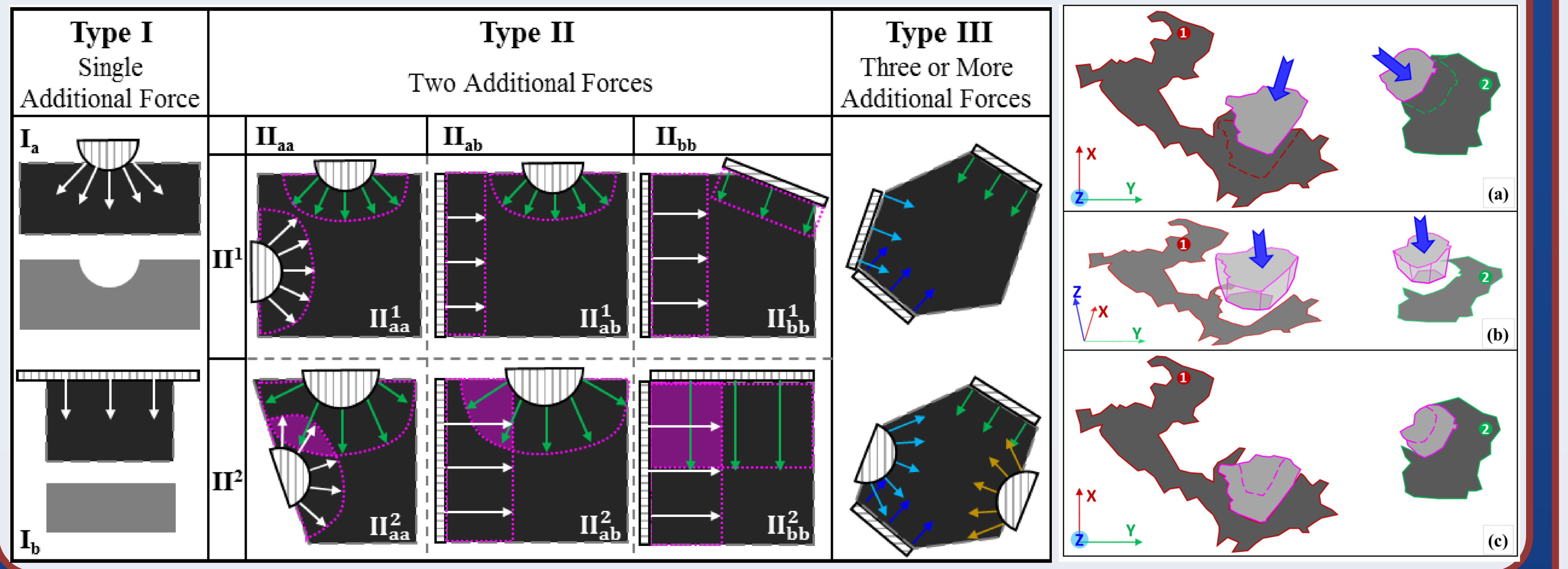

❖ Deformation Process of OM Particles

- 1. Both the solid kerogen and solid/quasi-solid bitumen are very soft under reservoir condition, compared to siliceous and carbonate minerals
- 2. A large number of OM-hosted pores are developed by thermal cracking and the kerogen and bitumen are hardened due to increase of carbon ratio
- 3. When the forces applied on OM alter (having additional forces), the porous OM is deformed
  - The original spherical pores are flattened
  - The OM frame is either bent, stretched, or shortened to match the pore geometry change
  - During the deformation of porous OM, the additional force is adsorbed and becomes smaller; thus the deformation may be limited in part of the OM

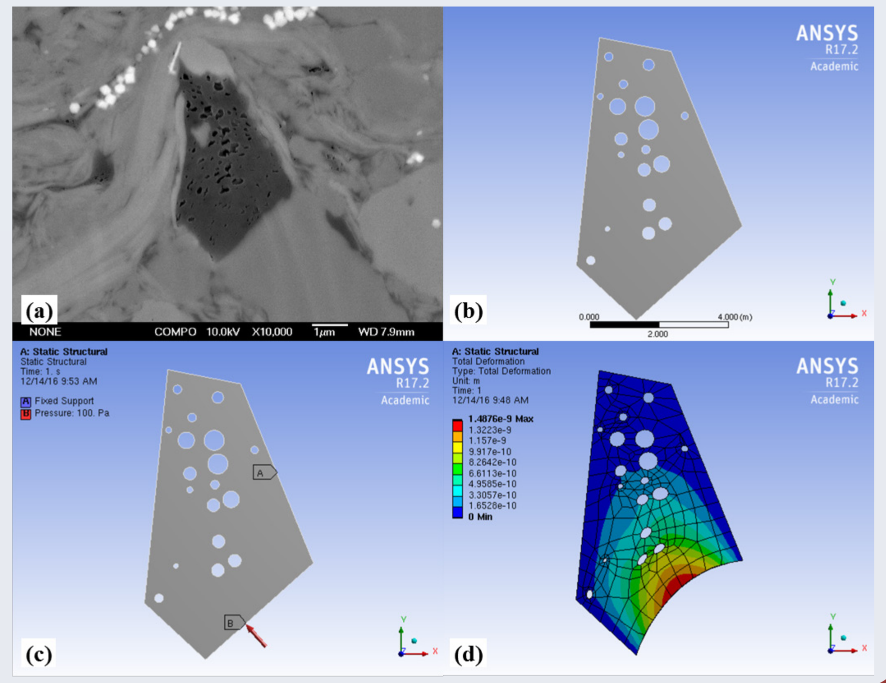

❖ Reference List

1. Dong T., et al., 2017, The impact of composition on pore throat size and permeability in high maturity shales: Middle and Upper Devonian Horn River Group, northeastern British Columbia, Canada
2. Loucks R., et al., 2009, Morphology, Genesis, and Distribution of Nanometer-scale Pores in Siliceous Mudstones of the Mississippian Barnett Shale
3. Milliken K., et al., 2013, Organic matter-hosted pore system, Marcellus Formation (Devonian), Pennsylvania
4. Klaver J., et al., 2015, BIB-SEM characterization of pore space morphology and distribution in postmature to overmature samples from the Haynesville and Bossier Shales
5. Jiao K., et al., 2014, The characterization and quantitative analysis of nanopores in unconventional gas reservoirs utilizing FESEM–FIB and image processing: An example from the Silurian Longmaxi Shale, upper Yangtze region, China
6. Peng S., et al., 2015, An Integrated Method for Upscaling Pore-Network Characterization and Permeability Estimation: Example from the Mississippian Barnett Shale
7. Schieber J., 2010, Common themes in the formation and preservation of porosity in shales and mudstones: Illustrated with examples across the Phanerozoic

❖ Estimation of the Initial Pore Size

Quantitatively estimating the decrease of pore size within OM is NOT easy even for the simplest deformation Type I. The major difficulty results from the unclearness of deformation process. Therefore, besides assuming the OM-hosted pores are spherical before deformation, another assumption concerning the deformation process should be made.

$$\frac{V_{sp}}{V_{el}} = \frac{1}{AR^2}\left(\frac{AR^2}{2} + \frac{AR}{4\sqrt{AR^2-1}}\ln\left(\frac{AR+\sqrt{AR^2-1}}{AR-\sqrt{AR^2-1}}\right)\right)^{1.5}$$

$$\frac{SA_{sp}}{SA_{el}} = 1$$

$$\frac{A_{sp,2D}}{A_{el,2D}} = \frac{AR}{2} + \frac{1}{4\sqrt{AR^2-1}}\ln\left(\frac{AR+\sqrt{AR^2-1}}{AR-\sqrt{AR^2-1}}\right)$$

$$PHI_{OM,2D,Init} = \frac{\frac{A_{sp,2D}}{A_{el,2D}}PHI_{OM,2D,De}}{1-PHI_{OM,2D,De}+\frac{A_{sp,2D}}{A_{el,2D}}PHI_{OM,2D,De}}$$

$$\frac{V_{sp}}{V_{el}} = AR$$

$$\frac{SA_{sp}}{SA_{el}} = \frac{4\sqrt{AR^2-1}}{2\sqrt{AR^2-1}+\ln\left(\frac{AR+\sqrt{AR^2-1}}{AR-\sqrt{AR^2-1}}\right)}$$

$$\frac{A_{sp,2D}}{A_{el,2D}} = AR$$

$$PHI_{OM,3D,Init} = \frac{\frac{V_{sp}}{V_{el}}PHI_{OM,2D,De}}{1-PHI_{OM,2D,De}+\frac{V_{sp}}{V_{el}}PHI_{OM,2D,De}}$$

	Deformation Process Assumption	AR Ave.	2-D OM Porosity	Sphere to Ellipsoid Vol. Ratio	Sphere to Ellipsoid SA Ratio	Sphere to Ellipsoid 2-D Area Ratio	Initial 2-D OM Porosity	Initial 3-D OM Porosity
Region R7	Constant Surface Area	1.650	0.371	1.073	1.000	1.239	0.422	0.388
	Constant Longest Principle Axis	1.650	0.371	1.650	1.094	1.650	0.493	0.493
Entire OM	Constant Surface Area	2.045	0.177	1.157	1.000	1.399	---	---
	Constant Longest Principle Axis	2.045	0.177	2.045	1.141	2.045	---	---

Sample A02

Method Limits: (1) Type I deformation; (2) only gentle deformation; (3) visible pores at 2-D FIB-SEM images; (4) pores within bitumen.

❖ Conclusion

- Organic matter (OM) deformation is approved using the features of OM-hosted pores observed on FIB-SEM images.
- After deformation, the size and direction of OM-hosted pores are not randomly distributed and the geometry tends to be flat.
- OM deformation is classified into different types.
- Heterogeneity of OM-hosted pore is affected by origin of OM-hosted pores, thermal maturity, OM Type, and OM deformation.